FUNDAMENTAL RESEARCH

For. Sci. XX(XX):1–15
doi: 10.1093/forsci/fxz085
Published by Oxford University Press on behalf of the Society of American Foresters 2020.
This work is written by (a) US Government employee(s) and is in the public domain in the US.

biometrics

Towards Spatially Explicit Quantification of Pre- and Postfire Fuels and Fuel Consumption from Traditional and Point Cloud Measurements

Andrew T. Hudak, Akira Kato, Benjamin C. Bright, E. Louise Loudermilk, Christie Hawley, Joseph C. Restaino, Roger D. Ottmar, Gabriel A. Prata, Carlos Cabo, Susan J. Prichard, Eric M. Rowell, and David R. Weise

Methods to accurately estimate spatially explicit fuel consumption are needed because consumption relates directly to fire behavior, effects, and smoke emissions. Our objective was to quantify sparkleberry (*Vaccinium arboretum* Marshall) shrub fuels before and after six experimental prescribed fires at Fort Jackson in South Carolina. We used a novel approach to characterize shrubs non-destructively from three-dimensional (3D) point cloud data collected with a terrestrial laser scanner. The point cloud data were reduced to 0.001 m^{-3} voxels that were either occupied to indicate fuel presence or empty to indicate fuel absence. The density of occupied voxels was related significantly by a logarithmic function to 3D fuel bulk density samples that were destructively harvested (adjusted R^2 = .32, P < .0001). Based on our findings, a survey-grade Global Navigation Satellite System may be necessary to accurately associate 3D point cloud data to 3D fuel bulk density measurements destructively collected in small (submeter) shrub plots. A recommendation for future research is to accurately geolocate and quantify the occupied volume of entire shrubs as 3D objects that can be used to train models to map shrub fuel bulk density from point cloud data binned to occupied 3D voxels.

Keywords: airborne laser scanning, Fort Jackson, prescribed fire, sparkleberry, terrestrial laser scanning

In wildland fires, fuel consumption is a major determinant of fire behavior and severity (Byram 1959), which are ecologically important for carbon and nutrient dynamics, soil erosion, vegetation recovery, and succession (Turner et al. 1997, Lentile et al. 2007, Keeley 2009, Sikkink and Keane 2012). Consumption is defined as the amount of live and dead biomass that is either pyrolyzed or combusted during a fire (Ottmar 2014). Because fuel consumption is a major determinant of heat release, smoke production, and pollutant emissions, characterizing fuel consumption and combustion by flaming and smoldering phases is necessary for modeling fire–atmosphere interactions and related smoke emissions (Potter et al. 2012, Ottmar et al. 2017, Prichard et al. 2019). Because of differences in fuel structure and suitability for combustion, fuel consumption is spatially heterogeneous and varies by fuel type from the canopy to the forest floor. Combustible fuels include (1) live and dead canopy fuels, composed of tree stems, branches, and needles; (2) ladder fuels such as vines, regenerating trees, or dead lower branches that connect surface fuels to canopy fuels; (3) understory shrubs and herbaceous (grasses, forbs); (4) surface fuels composed of coarse woody debris (CWD) and fine woody debris (FWD); and (5) forest floor fuels composed of a litter layer above a denser organic soil layer, termed duff (Davis 1959). In frequently

Manuscript received March 1, 2018; accepted December 6, 2019; published online January 22, 2020

Affiliations: *Andrew T. Hudak (ahudak@fs.fed.us) and Benjamin C. Bright (benjamincbright@fs.fed.us), US Forest Service, Rocky Mountain Research Station, Moscow, ID. Akira Kato (akiran@faculty.chiba-u.jp), Chiba University, Chiba, Japan. Louise Loudermilk (elloudermilk@fs.fed.us) and Christie Hawley (cmstegall.cfds@gmail.com), US Forest Service, Southern Research Station, Athens, GA. Joseph C. Restaino (restaino@u.washington.edu) and Susan J. Prichard (sprich@uw.edu), University of Washington, Seattle, WA. Roger D. Ottmar (rottmar@fs.fed.us), US Forest Service, Pacific Northwest Research Station, Seattle, WA. Gabriel A. Prata (gaprata@usp.br), University of São Paulo, Piracicaba, Brazil. Carlos Cabo (carloscabo.uniovi@gmail.com), University of Oviedo, Mieres, Spain. Eric M. Rowell (eric.rowell@gmail.com), Tall Timbers Research Station, Tallahassee, FL. David R. Weise (dweise@fs.fed.us), US Forest Service, Pacific Southwest Research Station, Riverside, CA.*

Acknowledgments: *This research was funded by Department of Defense Strategic Environmental Research and Development Program Project RC-2640: "Fundamental measurements and modeling of prescribed fire behavior in the naturally heterogeneous fuel beds of southern pine forests." Additional support was provided by Joint Fire Science Program Project 16-4-01-15: "Hierarchical 3D fuel and consumption maps to support physics-based fire modeling." We thank four anonymous reviewers and the Guest Editor for their valuable comments.*

burned ecosystems such as southern pine forests maintained using prescribed fires, a midstory and ladder fuels are almost entirely absent, so only ground, surface, and understory fuels typically combust, and as such, we focus on these fuels in this study.

Research on fuel consumption (available fuel) often reports consumption as the difference between total preburn fuel loading and total postburn fuel loading for a given prescribed burn management unit (Byram 1959, Wright 2013, Ottmar et al. 2016). Operational wildland fuel consumption models such as Consume and the First Order Fire Effects Model (FOFEM) estimate wildland fuel consumption by category (e.g., tree crowns, shrubs, herbs, downed wood by size class, litter, and duff) (Reinhardt et al. 1997, Prichard et al. 2007, Lutes et al. 2012, Prichard et al. 2014). However, further refinements are needed to spatially characterize fuel consumption to understand fine-scale fire effects (Hiers et al. 2009, Wiggers et al. 2013, O'Brien et al. 2016) and to provide more accurate estimates of pollutant emissions, many of which markedly vary between the flaming and smoldering phases of combustion (Urbanski 2014). For example, fuelbeds dominated by fine fuels such as litter, grasses, forbs, and shrub crowns generally burn mostly in the relatively short yet efficient flaming phase of combustion. In contrast, fuelbeds dominated by coarse wood and/or organic soils burn more in the longer-term, less efficient smoldering combustion phase with implications for soil heating and longer-duration smoke impacts (Haase and Sackett 1998).

Wildland fuels are virtually always highly heterogeneous in terms of composition, loading, and flammability (Keane et al. 2012, Keane and Gray 2013). Because the structure and complexity of fuel beds vary in space and time, so do fire behavior and fire effects at commensurate scales (Parsons et al. 2011). The complexity of wildland fuelbeds at multiple spatiotemporal scales greatly complicates their characterization, even at a single point in time for a single combustible material. In other words, spatial heterogeneity requires spatial characterization; high heterogeneity observed at the plot scale, for example, may appear as a homogenous repeating pattern at the stand scale. Although wildland fuels vary in three dimensions, as do fire behavior and fire effects (Loudermilk et al. 2012), no study to our knowledge has ever estimated consumption in 3D such that it could be functionally linked to fire behavior and effects.

Fuel and Consumption Measurements

Existing Methods

Direct measurement of consumption of heterogeneous, wildland fuelbeds in situ and in 3D is still beyond current technological capabilities. Studies that have successfully estimated fuel consumption have done so indirectly, by one of three methods. The active fire method measures the energy release of burning fuel, which has been shown to be linearly related to fuel consumption as shown by small fire experiments (Byram 1959, Wooster et al. 2005, Smith et al. 2013). The retrospective method measures immediate postfire white ash content, the first-order product of combustion, which has been shown to be linearly related to consumption (Smith and Hudak 2005, Hudak et al. 2013, Ottmar et al. 2016). The traditional and most applied method is to measure the fuelbeds in situ, pre- and postfire, and then subtract the latter from the former to calculate consumption (Campbell 1959, Hough 1968, van Wagner 1972, Hough 1978, Brown et al. 1991, Scholl and Waldrop 1999, Sullivan et al. 2003, Hollis et al. 2010, Wright 2013, Ottmar et al. 2016). However, by any of these existing methods, it is impractical to resolve consumption of all component materials at the scales at which they vary in heterogeneous, wildland fuelbeds. This problem is akin to the challenge of estimating forage use, which has been studied extensively in range management (Heady 1949, Southern Forest Experiment Station 1959).

Some traditional fuel measurement methods can be colocated to provide direct measures of consumption, such as the wire-log method (Hedin and Turner 1977, Brown et al. 1991, Albini et al. 1995, Prichard et al. 2017), to estimate consumption of logs, and the duff pin method (Beaufait et al. 1975, Lewis et al. 2011) for forest floor consumption. However, destructive sampling techniques that harvest, dry, and weigh fuels before the fire necessarily prevent postfire measurements at the same locations. Because the locations of pre- and postfire destructive harvest or "clip" plots must differ, consumption estimates derived from paired pre- and postfire fuel measurements will have a coarser spatial resolution (Hudak et al. 2017).

Point Cloud Methods

New developments in remote sensing technology involving quantitative interpretation of point cloud datasets collected with light detection and ranging (lidar) or similar technologies hold promise for fine-scale, in situ characterization of fuels and consumption (Seielstad and Queen 2003, Hiers et al. 2009, Loudermilk et al. 2009). Airborne lidar, also known as airborne laser scanning (ALS), is used widely and operationally in forest inventory for characterizing forest structure (Hudak et al. 2009). Comparing pre- and postfire ALS was demonstrated as a feasible means to characterize canopy consumption in the New Jersey pine barrens burned with prescribed crown fires (Mueller et al. 2017), and McCarley et al. (2017a, b) mapped canopy cover change because of fire, bark beetles, and harvest using pre- and postfire ALS in central Oregon. ALS provides landscape-level coverage from a vertical (nadir) or

Management and Policy Implications

Public health concerns stemming from smoke emissions from prescribed fires are a major constraint for land managers on when, where, and how to burn. Fire and fuel managers would benefit greatly from remote sensing methods to quantify fuels loads, one of the major determinants of whether to prescribe a fire, and under what conditions. Methods that account for fuel heterogeneity are needed to do this more reliably because current operational fire and smoke models assume homogeneous fuel distributions. Although fire behavior, fire effects, and smoke emissions from fires relate to fuel structure and composition, they even more directly relate to fuel consumption. Estimation of fuel consumption requires research beyond quantification of fuel loads, whether prefire for purposes of fuel and fire planning, or postfire as a way to assess and predict fire effects. Our approach and findings advance the characterization of spatially complex shrub fuels in 3D, at the scales at which they vary using terrestrial laser scanning technology, so we can enhance the capabilities of fire and smoke models needed by managers and planners. Improved quantification of fuels and fuel consumption also will provide better, spatially explicit information to fire, fuel, and smoke managers and modelers, and policymakers.

high oblique (e.g., high scan angle) perspective, albeit at a reduced point density compared to terrestrial laser scanning (TLS) data.

At a finer scale, TLS provides denser 3D point cloud characterization from a horizontal or low oblique (e.g., from a boom lift) perspective. TLS of understory vegetation/fuel has been applied before and after prescribed understory fires in a longleaf pine ecosystem (Loudermilk et al. 2009, Rowell et al. 2016a, b) and to describe fuels in Douglas-fir (Seielstad et al. 2011). Although TLS provides a higher spatial resolution than ALS to differentiate between overstory, understory, and canopy fuels, the spatial extent is usually limited to that of a typical forest inventory plot, with at least two scans from different view perspectives required (Olsoy et al. 2014), and even five scans are needed in forests to overcome occlusion by tree trunks or other objects obstructing the view (Stovall and Shugart 2018).

Justification and Objectives

Why is 3D fuel information needed? Fire scientists and managers input fuel information into fire and smoke models to better understand expected fire behavior, smoke emissions, and fire effects, all of which have important implications for fire and fuel managers (Parsons et al. 2017). That these data must be in 3D is critical to provide the complexity needed for quality fire behavior simulations (Rowell et al. 2016a). Indeed, it is the fuel leg of the fire behavior triangle (also composed of topography and weather) that is often described as the only component that can be manipulated (Parsons et al. 2016). The minimum observational requirements for fuels and consumption vary greatly across the spectrum of fire and smoke models—from relatively simple point-based operational models such as BehavePlus (Andrews et al. 2005), Consume (Prichard et al. 2007), and FOFEM (Reinhardt 1997, Lutes et al. 2012) to operational models that spread fire across landscapes such as FARSITE and FlamMap (Stratton 2006), to complex physics-based models such as WFDS (Mell 2007, 2009), FIRETEC (Linn et al. 2002, 2005), and WRF-SFIRE-CHEM (Mandel et al. 2011, 2014) that simulate fire behavior in 3D. These latter, physics-based models resolve combustion within 3D gridded meshes and require 3D fuel inputs at fine resolutions (generally submeter to 5-m mesh size).

The overarching goal of this study was to measure fuels and estimate consumption in fuelbeds in 3D at a resolution commensurate with fuel observations collected pre- and postfire on experimental prescribed burns. For this study, we focused on understory shrub fuels. We collected TLS point clouds and destructively harvested fuel biomass, both in 3D, before and after burning to quantify consumption in 3D. We also compared 3D shrub fuel consumption estimates to those derived from traditional destructive samples collected pre- and postfire.

Methods

Study Area

Our study was located at Ft. Jackson, an Army Base located east of Columbia, South Carolina (Figure 1), in southern pine forests dominated by slash pine (*Pinus elliottii*) and longleaf pine (*Pinus palustris*). Frequent prescribed burning (2–5-year fire rotation interval) is used to limit understory growth and surface fuel accumulations to facilitate military training and to promote dominance of fire-dependent longleaf pine over less fire-resistant slash pine (Regional Working Group 2009). Other important management objectives are to manage timber resources and conserve habitat for the red-cockaded woodpecker (*Picoides borealis*), listed as an endangered species that requires these frequently burned southern pine forests for nesting and foraging.

Field Measurements

Sparkleberry (*Vaccinium arboretum* Marshall) is the predominant shrub species in the plots burned for this study and was the only species targeted for sampling. At Ft. Jackson, it is often the major understory shrub associated with longleaf pine. A bulldozer was used to establish firebreaks to delimit the experimental burn units, each ~0.16 hectare in size, or just large enough to encompass a 40-m × 40-m area designated for pre- and postfire field sampling and TLS (Figure 1). The plots had been last burned 2 years prior, in the growing season. All burn units were selected for having sparkleberry shrub coverage, which was unevenly distributed as individual plants or in clumps of varying size (Figure 2). Within each burn unit, paired pre- and postfire sparkleberry shrubs subjectively selected for proximity and similar stature were harvested for 3D biomass measurement within a 0.5-m × 0.5-m destructive sample (i.e., clip) plot. Four paired shrub plots (four prefire and four postfire) per burn unit were clipped beginning from the shrub top (<2 m) and clipping at 0.1-m vertical intervals down to ground level (Figure 3). All shrub material was clipped, bagged, and labeled separately by vertical stratum. Frame design, construction, and 3D sampling protocol are further described in Hawley et al. (2018).

In addition to the paired sparkleberry shrub clip plots, four paired clip plots (four prefire and four postfire), also 0.5-m × 0.5-m in size horizontally (0.25 m^2), were established to estimate fuel consumption of shrubs, grass, fine downed woody debris (<7.62 cm diameter), litter, and duff in 2017. Based on a preliminary analysis of the 2017 samples, the plot size was quadrupled and the sampling effort doubled in 2018 to overcome higher-than-anticipated fuel variation; i.e., eight prefire and eight postfire 1-m × 1-m clip plots were established to estimate fuel consumption of shrubs, grass, and fine downed woody debris in 2018. The paired plots were laid out systematically at 5-m (2017) or 8-m (2018) intervals, with 2 m (2017) or 6 m (2018) separating each pre- and postfire pair.

Pre-and postfire material collected from all clip plots was weighed and oven-dried at 70° C for 48 h to determine dry biomass weight. Fuel consumption of the shrubs, grass, and small down woody debris was calculated by subtracting the prefire biomass from the postfire biomass for each fuelbed category.

Because of the high variability in litter and duff depth observed in 2017, litter and duff consumption in 2018 was measured using 16 consumption pins per paired consumption plot. The pins were pushed into the litter and duff layer with the head of the pin flush with the top of the litter. After the fire, each pin was located, and total litter and duff prefire depth and postfire depth were measured. Using a representative bulk density for the litter and duff of the region (Ottmar et al. 2003), the prefire depth and postfire reduction in the litter and duff were converted into biomass.

Fuel moisture sampling was initiated 2 h before ignition. Shrubs, grass, downed woody material, litter, and duff moisture samples were collected, with the finer fuel fractions most amenable to drying collected later, i.e., closer to the time of ignition. All material was bagged, weighed, and then oven-dried at 70° C for 48 h to determine the moisture content for each fuelbed category.

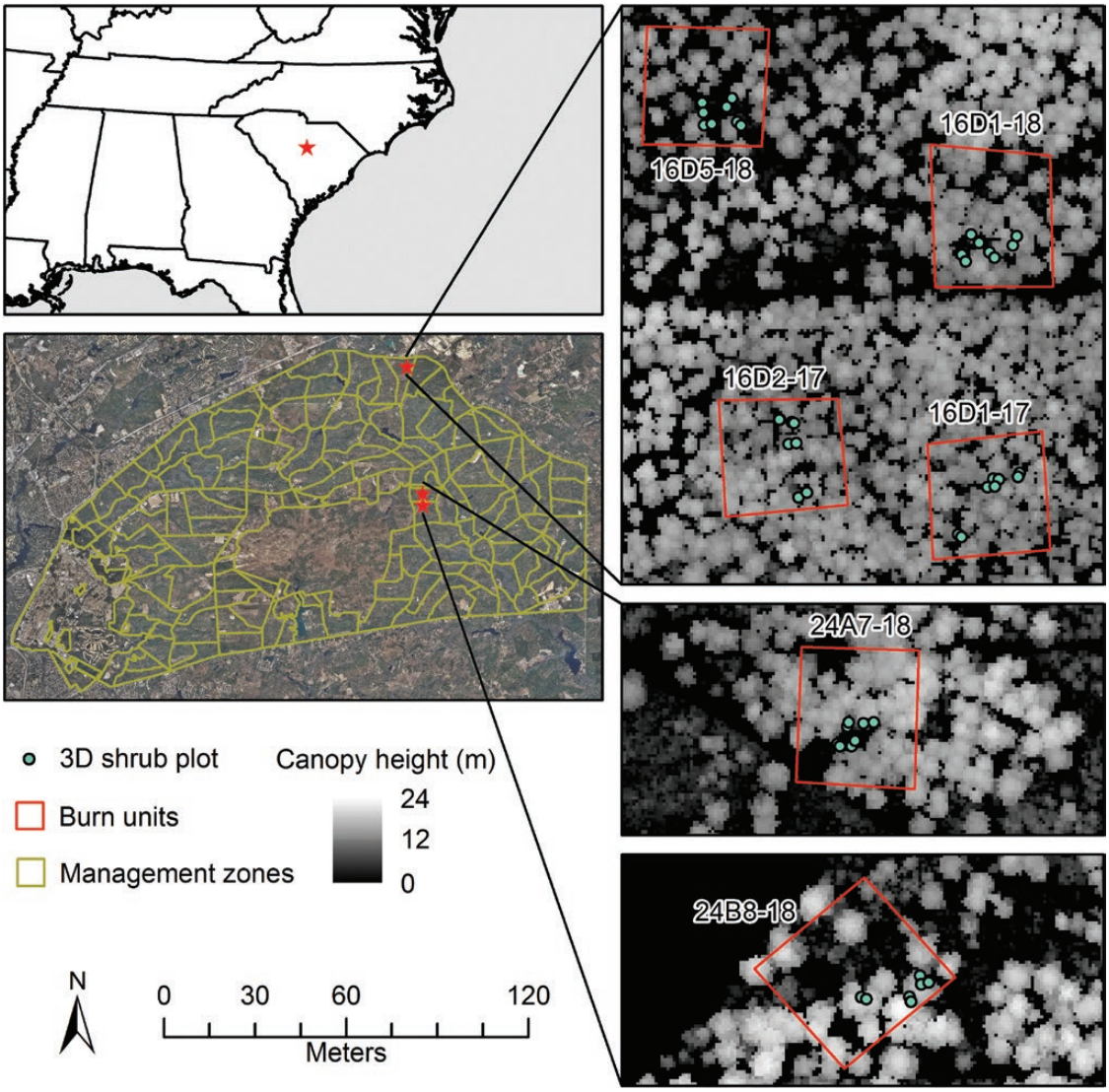

Figure 1. Location of six experimental burn units situated within management zones 16D, 24A, and 24B at Ft. Jackson Army Base, South Carolina, USA. Background image illustrates individual tree crowns from the canopy height model (CHM) interpolated from airborne laser scanning (ALS) data at 0.5-m × 0.5-m resolution.

Within each burn 40-m × 40-m unit, metal conduits were installed to demarcate the four corners of a 30-m × 30-m square for focusing TLS point cloud data collections. Within each large square, additional conduits were used to mark the corners of smaller, nested squares of 10-m × 10-m and 4-m × 4-m targeted for more intensive scanning in 2017. In 2018, rather than marking smaller nested squares, conduits were used to mark sparkleberry shrub plots, selected for more intensive scanning and destructive sampling, and distributed such that the scans were spatially nested within the 30-m × 30-m largest squares similarly to 2017. Each conduit was geolocated with a resource-grade Global Navigation Satellite System (GNSS) receiver (Geo7X, Trimble Inc.)[1] with real-time differential correction capability. Geolocations were recorded for all nested square plot corners marked with metal conduit, as were the paired clip plots, paired sparkleberry shrubs selected for 3D fuel sampling, and trees. The recorded tree attributes were: species, status (live, unhealthy, dead), diameter at breast height (dbh), height, height to crown, and crown diameter (major and minor axes).

TLS

The TLS used was an LMS 511 (SICK Inc.).[1] The horizontal line scanner of the laser sensor was placed vertically on the rotation table, which rotated 360° to capture the three-dimensional point cloud data. The portable TLS system was set up on a tripod and easily carried to more convenient positions in the burn unit affected less by tree boles or dense shrub clumps that obstructed the view for data collection. The sensor itself was a line sensor, which meant the laser shot in one dimension. The sensor was set to scan vertically from bottom (ground) to top (sky) while mounted on top of a turntable that was rotated 360° horizontally for every scan. The geolocation of the TLS for a given scan was set to zero initially; i.e., with a starting azimuth of 0° horizontally and a starting zenith of 0° vertically. The 3D point cloud data were created without a compass because the TLS was accurately calibrated horizontally and vertically, and the horizontal degree was accurately registered by the encoder as the turntable rotated. The TLS recorded 3D point locations with intensity values (strength of laser returns) normalized to

Figure 2. Prefire coverage of predominantly sparkleberry shrubs in (A) burn unit 16D1-17 and (B) burn unit 16D2-17, 2 years after the most recent burn.

8-bit unsigned values (0–255), but because intensity values did not represent actual object reflectance, they were ignored in this study.

Scans at each plot corner plus the mid points between plot corners along the square boundary provided a minimum of eight scans for each of the nested square plots scanned in 2107. Based on a preliminary analysis of 16 sparkleberry shrubs selected for 3D fuel sampling in 2017, a minimum of two scans were collected surrounding each of the sparkleberry shrubs selected for 3D fuel sampling in 2018. In some cases, three to four scans were required to ensure that shrubs were scanned to overcome occlusion by other objects and clearly see the targeted shrubs in the point clouds, along with the metal conduits marking their locations. The shrubs selected for 3D sampling were spatially clustered such that the distribution of the scans was spatially nested within the larger burn unit in 2018 like in 2017. Around the periphery of an area to be scanned, four to eight reflective targets were positioned to remain stationary and provide relative tie points for merging point clouds from separate scans as the TLS was moved around the plot. Although commercial TLS have ready-to-use, specialized software to merge the scans, this customized TLS did not, so an automated merging algorithm was developed for this study, as described below.

Point Cloud Data Processing

Georegistration

Preprocessing was necessary to match point cloud datasets in the same georeferenced coordinates. The TLS x, y, z data were referenced initially to the 0, 0, 0 origin (the initial sensor location). Treetop locations were used to georegister the TLS data to the ALS data in real-world coordinates. First, a digital surface model (DSM) was created from the maximum height of discrete points within 0.25-m × 0.25-m resolution grid cells. Second, Gaussian filtering

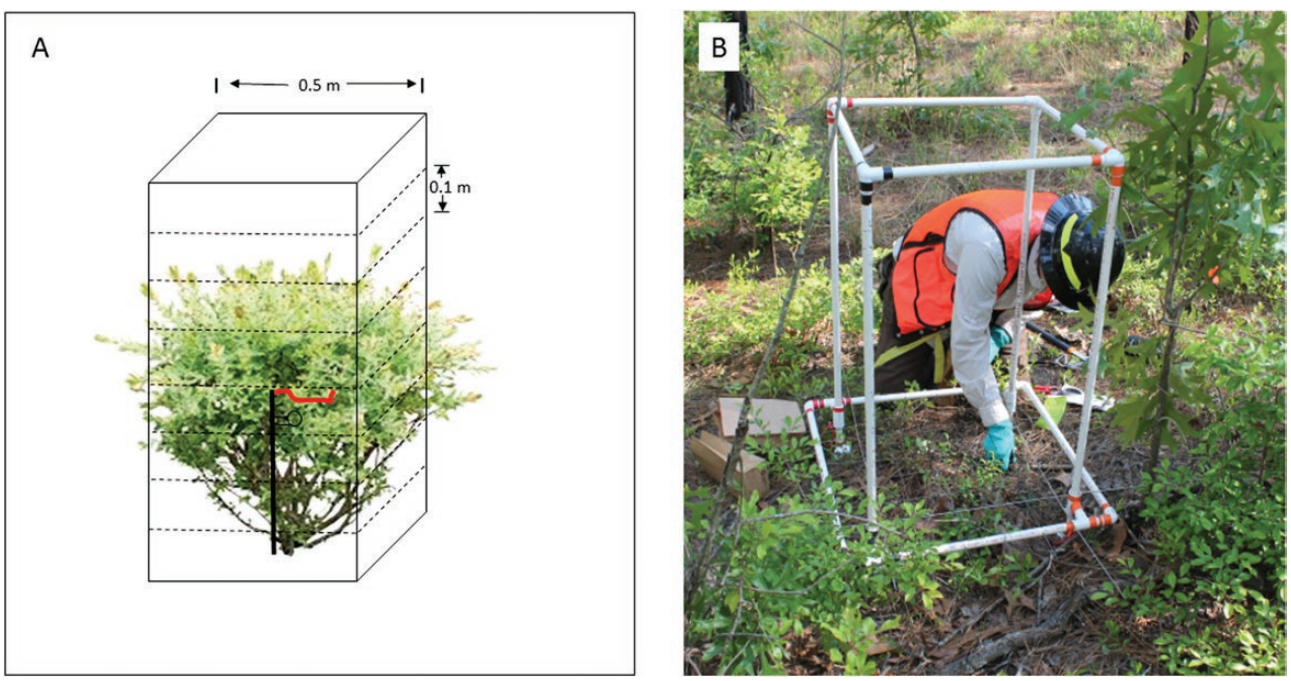

Figure 3. Sparkleberry shrub clipped at 0.1-m vertical intervals from the top down to ground level within a 0.5-m × 0.5-m sample plot (A) in theory and (B) in practice.

was applied to smooth the DSM, and all peaks were automatically identified using local maxima filtering within a 5 × 5 moving window. Third, treetop locations were used to shift and rotate the DSM to fit the treetops in a 0.5-m × 0.5-m georectified canopy height model derived from the ALS data, collected on November 21, 2015 by the Army Geospatial Center, as part of the BuckEye mission, using an Optech ALTM Gemini sensor. The ALS point density averaged 8.7 returns m^{-2}. The TLS point clouds were height normalized by subtracting the 0.5-m × 0.5-m digital terrain model derived from the ALS.

Shrub Plot Location Adjustment

Using the las file viewer of LASTools (Isenburg 2018), the point cloud data from the merged scans were viewed in the vicinity of the metal conduits marking the sparkleberry shrubs selected for 3D sampling; the conduit marking the shrubs provided a visible feature in the TLS point clouds to ensure accurate coregistration. Adjusting the conduit locations was determined to be essential, as the geolocation errors of the conduit positions collected under forest canopy, despite real-time and postprocessing differential correction, were often as large as or sometimes larger than the size of the 0.5-m × 0.5-m 3D shrub sampling frame.

Conduit Removal

To increase the accuracy of shrub fuel load estimates, TLS points reflecting off the metal conduits were removed. Virtual conduit removal was performed using methods built upon previous work for automatic pole-like object detection (Cabo et al. 2014, 2018). These methods are based on the isolation of some parts of the poles (conduits in this case) and were applied to subsets of the point clouds around the adjusted locations of the conduits. First, the points belonging to each subset were voxelized; a voxel is analogous to a pixel but represents a volumetric space in a three-dimensional (3D) regular grid. Voxels then were grouped according to their proximity and vertical continuity. After that, and not assuming that the conduits were completely vertical, an initial directrix line of the conduit was computed using a principal-component analysis of the x, y, z coordinates. From this line, noise and artifacts around the conduit were detected and removed. This last step was performed iteratively, recalculating the directrix line of the conduit. Finally, the results were validated visually before removal of the TLS points reflected off the conduits.

Voxelization

TLS point densities differed as an artifact of the different sensor scanning locations rather than the vegetation/fuel structure of interest. Upon merging the TLS data from the different scans, there was duplication of 3D point distributions from some objects scanned from different angles. To minimize the effect of duplication, 0.1-m × 0.1-m × 0.1-m voxels (i.e., 0.001 m^{-3}) were generated. Voxels containing one or more 3D points were assigned a value of 1 to indicate fuel presence; otherwise voxels were assigned a value of 0 to indicate fuel absence. This greatly reduced the file size of the 3D fuel presence maps pre- and postfire, relative to the original TLS data volume. Only TLS points in the vertical space occupied by shrubs, between 0.1 m and 2 m above ground level, were included in the voxelization. Consumption maps were generated at 1 m^{-3} resolution by tallying the difference in occupied 0.001 m^{-3} voxels between the pre- and postfire maps of fuel presence.

Shrub Fuel Bulk Density Modeling

At each 3D shrub clip plot location, occupied voxels were tallied within a virtual 0.5-m × 0.5-m × 2-m rectangular frame superimposed on the point cloud, for comparison with measured shrub fuel bulk density. Models predicting pre- and postfire shrub fuel bulk density were fitted based on the 2018 data only, because in 2017 the TLS point densities at the sparkleberry shrubs selected for 3D fuel sampling were insufficient to reliably see the metal conduits, as in 2018. Because the shrub fuel densities were not normally distributed, Spearman rank (rather than Pearson) correlation and adjusted R^2 were calculated to assess the strength and significance of relations. Predictive models were fitted, residuals inspected, and statistics generated using R statistical software (R Core Team 2015).

Results

Traditional Measurements

All six replicate burn units had similar overstory, understory, and surface fuel conditions. The first two units were burned on May 9, 2017 in the late morning (16D1-17) and early afternoon (16D2-17); winds were light and from the northwest (Figure 4). In 2018, four plots were burned under light southwest winds on successive days: May 1 (24B8-18) and May 2 (24A7-18) in the afternoon, and May 3 in the morning (16D1-18) and afternoon (16D5-18). Mean fuel moisture contents were relatively low for litter and FWD, intermediate for duff, and high for the mostly live herbaceous and shrub fuels in particular, which was typical since this was the spring growing season (Blackmarr and Flanner 1968) (Table 1). The Spearman rank correlation between fuel moisture content and consumption was significant ($\rho = -0.68$, $P < .001$). Surface and ground fuels were mostly composed of 2 years of accumulated needle fall that made litter the largest contributor to consumption, followed by duff and FWD (Table 1, Figure 5). Herbaceous fuel was a minor contributor to consumption, whereas calculated shrub consumption was negative because measured shrub fuel loads were higher postfire than prefire at half of the burn units (Table 1, Figure 5). Duff was the largest fuelbed component both pre- and postfire in this fire-maintained southern pine ecosystem, followed by litter, FWD, and lastly the herbaceous and shrub fuels composed of mostly live biomass (Figure 5).

A large coefficient of variation provides further evidence that shrub fuels and consumption were the least reliably estimated of any fuelbed component by the traditional 2D method (Table 1, Figure 5). Destructive fuel measurements cannot be colocated, making traditional consumption measurements particularly problematic in the case of patchy shrub fuels having inherently high spatial variability in 3D. Moreover, consumption of fine fuel elements of the shrubs (leaves and twigs) varied widely within and between shrubs and shrub clumps from very incomplete, in which leaves were merely scorched, to virtually complete consumption where only charred larger stems remained (Figure 6).

Point Cloud Measurements and 3D Fuel Sampling

The TLS point clouds provided colocated 3D representations of overstory and understory canopy structure pre- and postfire (Figure 7). Treetops in the canopy height model (CHM) derived from the merged scans were coregistered to the ALS-derived CHM with higher accuracy in the 2D plane (mean root mean square error

Figure 4. Prescribed surface fire burning through burn unit 16D2-17.

Table 1. Prefire, day-of-burn fuel moisture content (percent) and consumption (g m^{-2}) by fuelbed variable measured via traditional methods, summarized for the six burn units.

Fuel variable	Fuel moisture (percent)					Consumption (g m^{-2})				
	Mean	SD	CV	Min	Max	Mean	SD	CV	Min	Max
Coarse woody debris	45.7	–	–	45.7	45.7	91.9	183.8	2.0	0.0	367.6
Fine woody debris	13.3	2.6	0.2	9.5	15.8	269.8	260.1	1.0	48.1	761.4
Shrubs	193.4	17.7	0.1	175.2	211.8	–25.8	221.8	–8.6	–353.7	329.5
Herbaceous	107.7	83.3	0.8	20.4	205.3	18.9	31.0	1.6	0.0	76.2
Suspended litter	9.6	2.0	0.2	7.5	11.8	19.1	3.9	0.2	15.7	24.7
Litter	8.1	2.8	0.3	4.3	10.6	1,287.7	748.4	0.6	769.4	2,675.6
Duff	55.2	32.4	0.6	25.7	110.8	514.7	522.3	1.0	147.6	1,432.4
Total	–	–	–	–	–	2,053.4	1,217.2	0.6	1,331.0	4,516.5

Note: Fine woody debris included 100-h, 10-h, 1-h fuels, and pine cones. Herbaceous fuels included grasses and forbs. Coarse woody debris, or 1,000-h fuels, were sampled in only one burn unit (24B8-18). Suspended litter (litter caught in shrubs above ground) was another minor fuelbed component that was completely consumed. Shrub consumption was unrealistically negative at three burn units where measured shrub fuels were higher postfire than prefire (Figure 5). CV, coefficient of variation; SD, standard deviation.

[RMSE] = 0.45 m) than in 3D (mean RMSE = 0.91 m), which may be attributable in part to 2–3 years of tree height growth between the 2015 ALS acquisition and the 2017–18 TLS collections (Table 2). At the two 2017 burn units, the maximum tree height measured in the field was 19.9 m, the mean tree height was 11.5 m (SD = 3.6 m), and the mean crown base height was 7.1 m (SD = 2.3 m). The maximum tree height measured with ALS was 23.7 m in burn unit 24B8-18, and in no burn units did it exceed 24 m (Figure 1). Sparkleberry shrubs at the 48 small 3D shrub clip plots averaged 1.0 m (SD = 0.3 m) in height and did not exceed 2 m (maximum = 1.7 m); therefore, the understory shrub canopy could be easily separated from the overstory tree canopy by considering only points <2 m above ground.

The resource-grade GNSS used reported a horizontal precision of 0.2–0.5 m, yet the accuracy of the recorded metal conduit geolocations marking the 3D shrub clip plots was worse, averaging 0.77 m (SD = 0.53 m), as calculated from how far the 32 metal conduit geolocations in 2018 were adjusted after viewing them in the TLS point cloud. The density of voxels occupied by TLS points was significantly related to both pre- and postfire shrub fuel bulk density at the 32 small 3D shrub plots measured in 2018, by a logarithmic relation (Figure 8). Excluding the TLS points reflected from the metal conduits improved the prefire model R^2 from 0.33 to 0.35 and the postfire model R^2 from 0.24 to 0.31. The mean shrub fuel bulk density due to consumption decreased from 556 to 379 g m^{-3} (31.8 percent), whereas occupied voxel density decreased

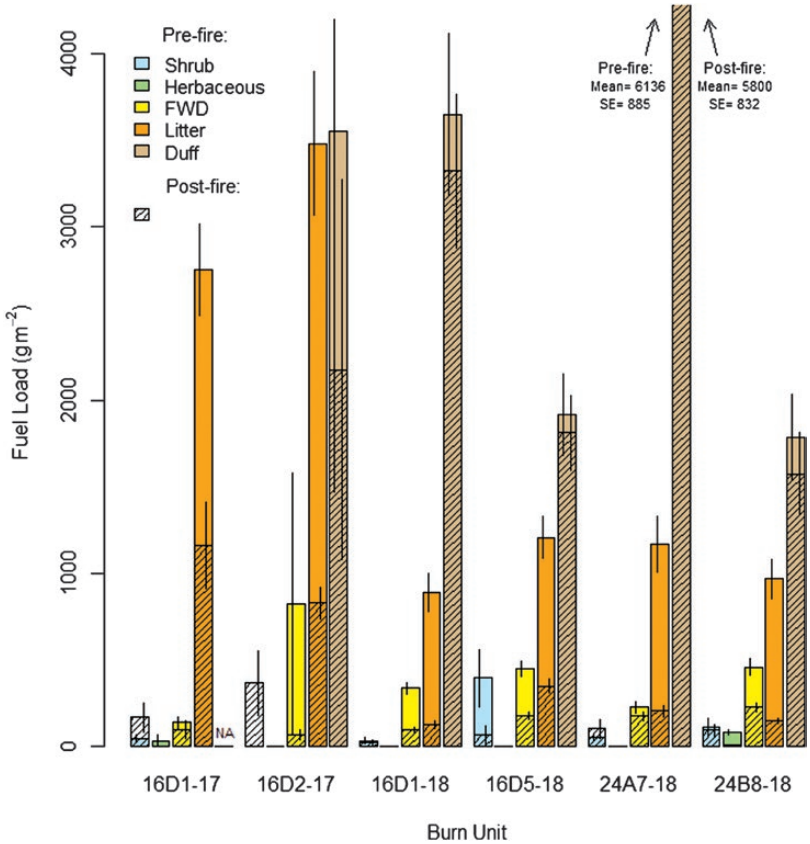

Figure 5. Mean (±SE) fuel loads prefire (colored) and postfire (hatched) for the five primary fuelbed components measured at six replicate burn units via traditional methods. The difference between mean pre and postfire fuel loads represents consumption. Note that postfire shrub fuel load exceeded prefire shrub fuel load at three burn units (i.e., negative consumption). See Table 1 for consumption estimates of all fuelbed components.

from 850 to 725 m^{-3} (14.7 percent). Shrub fuel bulk density and occupied voxel density both decreased because of the fire such that the best-fit lines had very similar shapes despite the high variability in these 0.5-m × 0.5-m × 0.1-m voxel-level observations around the best logarithmic fits (adjusted R^2 = .34 prefire and 0.30 postfire; see Figure 8); therefore, a single equation was fit to all pre- and postfire observations combined (Figure 8) to yield Equation 1:

$$y = 199.8768 \times \ln(x) - 323.5209 \quad (1)$$

where the dependent variable y denotes occupied voxel density (m^{-3}), and the independent variable x denotes shrub fuel bulk density (g m^{-3}). This combined logarithmic fit in Equation 1 was then algebraically inverted to yield:

$$x = e^{[(y+323.5209)/199.8768]} \quad (2)$$

whereby applying Equation 2, shrub fuel bulk density (x) was predicted from occupied voxel density (y) both pre- and postfire across the full extent of the TLS point clouds for all burn units. Fuel consumption was subsequently calculated as the difference between the pre- and postfire fuel bulk density maps for the six burn units (Figure 7).

2D (Traditional) versus 3D (Point Cloud) Estimates

Shrub consumption was of most interest for our study, given it was the fuelbed component most amenable to measurement in 3D. Although the measurement units differed between the 2D (g m^{-2}) and 3D (g m^{-3}) shrub fuel and consumption estimates, in this study the 3D estimates could be directly compared to the 2D estimates because the mean shrub height was 1 m across the six burn units (i.e., 1 g m^{-3} × 1 m = 1 g m^{-2}). The mean shrub fuel load estimated by the 2D traditional method compared to the 3D point cloud method was lower prefire (2D: 106.7 g m^{-2}; 3D: 111.8 g m^{-3}) but higher postfire (2D: 132.5 g m^{-2}; 3D: 74.2 g m^{-2}). The mean shrub consumption by the 2D traditional method was unrealistically negative (–25.8 g m^{-2}) and extremely variable (CV = –8.6, negative because the mean was negative), whereas by the 3D point cloud method, the mean shrub consumption (37.6 g m^{-3}) was reasonable and stable (CV = 0.4) across the six replicate burn units (Table 3). The physically impossible negative consumption estimates at half of the burn units provide strong evidence of under-sampling by the traditional method (Tables 1 and 3, Figure 5).

Discussion

Spatially Explicit Estimation of Consumption

The high resolution of TLS and ability to colocate pre- and postfire measurements using non-destructive point cloud data underpin their superiority over traditional methods for estimating shrub fuel consumption in a spatially explicit manner across the broad extent of prescribed burns. Nevertheless, efficient destructive sampling is required to construct a robust empirical model needed to convert occupied voxel counts to physical estimates of fuel bulk density. This is a critical consideration if only for the shrub fuel

Figure 6. Three selected sparkleberry shrubs marked with metal conduit prior to harvesting in 3D destructive sample plots (A) prefire; (B) postfire, where the combustible fine fuels were partially consumed and partially scorched; or (C) postfire, where the combustible fine fuels were completely consumed.

component, as demonstrated by sampled shrub fuels in this study. Although our voxelization approach based on 32 shrub fuel plots was significant, the functional relation between shrub fuel bulk density and occupied voxel density that underlies the predictive shrub fuel maps was noisy (Figure 8). Clustering TLS collections in near proximity to the small shrub clip plots, and, later, adjusting their locations by directly viewing the metal conduits in the point clouds, proved essential for overcoming the geolocation errors of the resource-grade GNSS equipment used. For most forestry applications this would be sufficient but, for this specialized, cubic decimeter 3D matching analysis, proved only marginally adequate. High geolocation accuracy, as is achievable using survey-grade GNSS equipment, may be essential for replicating this method if one were to forego using metal conduits or similarly identifiable features, although the overstory canopy can still impede the ability to achieve survey-grade (<0.02 m) GNSS accuracy (Andersen et al. 2009, Valbuena et al. 2010). If achieved, then other factors could measurably affect comparisons between pre- and postfire 3D fuel maps to estimate consumption, such as altered shapes of fuel elements after partial consumption or scorching from the fire. Wind was another factor that contributed to noise in the TLS point cloud data in this study.

Frequent prescribed fires carried out every 2–4 years to limit shrub growth and promote longleaf pine regeneration might be thought to have a homogenizing effect on fuel distributions across burn units. However, observed variability in fuel loads of most fuelbed components was large at the six burn units (Table 1, Figure 5), which may be in part a legacy effect of a prolonged period of fire exclusion (Kreye et al. 2014). The spatial distributions of surface fuels are inherently heterogeneous (Hiers et al. 2009, Loudermilk et al. 2009, Keane et al. 2012, Keane and Gray 2013), which likely affects consumption at this same scale and, in turn, fire behavior (Loudermilk et al. 2012). Such high spatial variability confounds traditional measurements of consumption with paired plots having pre- and postfire locations that necessarily differ, even if by only 2 m. Forest floor consumption pins, as were used in 2018 to determine litter and duff consumption, have the advantage of colocation, rather than paired pre- and postfire clip plots, as were used in 2017, which are necessarily placed at different locations. Only at burn unit 24B8-18 was CWD encountered in the systematic sampling; had CWD been more common in these burn units because of less frequent burning, pre- and postfire measures of CWD along fuel transects would need to be added to estimate total consumption. The wire-log method would provide colocated consumption measures at specific locations (Sandberg and Ottmar 1983).

This study focused on shrub fuel characterization and consumption, but shrubs were a relatively minor component of these mixed, heterogeneous fuelbeds. If fuel consumption is to be compared to energy release or other aspects of fire behavior, then pre- and postfire measurements of all the surface fuel components are required to estimate consumption, because fire behavior measurements cannot be easily partitioned by fuel categories that are simultaneously burning.

Point Cloud Sensors

In this study, shrub fuel was the only fuel component with a vertical component amenable to characterization with TLS. Had there been more herbaceous (grass and forb) fuel in this study's burn units, other data besides TLS may have been needed to separate shrub from herbaceous fuels (Mutlu et al. 2008). Bright et al. (2016) demonstrated that point clouds derived from digital stereo photographs collected from close range, like the TLS, can be used to classify plant functional types. Point-cloud-based approaches as presented here could be scaled and applied to crown fuels; tree crowns are larger objects with more combustible fuel, increasing the utility of ALS for estimating canopy fuels and consumption.

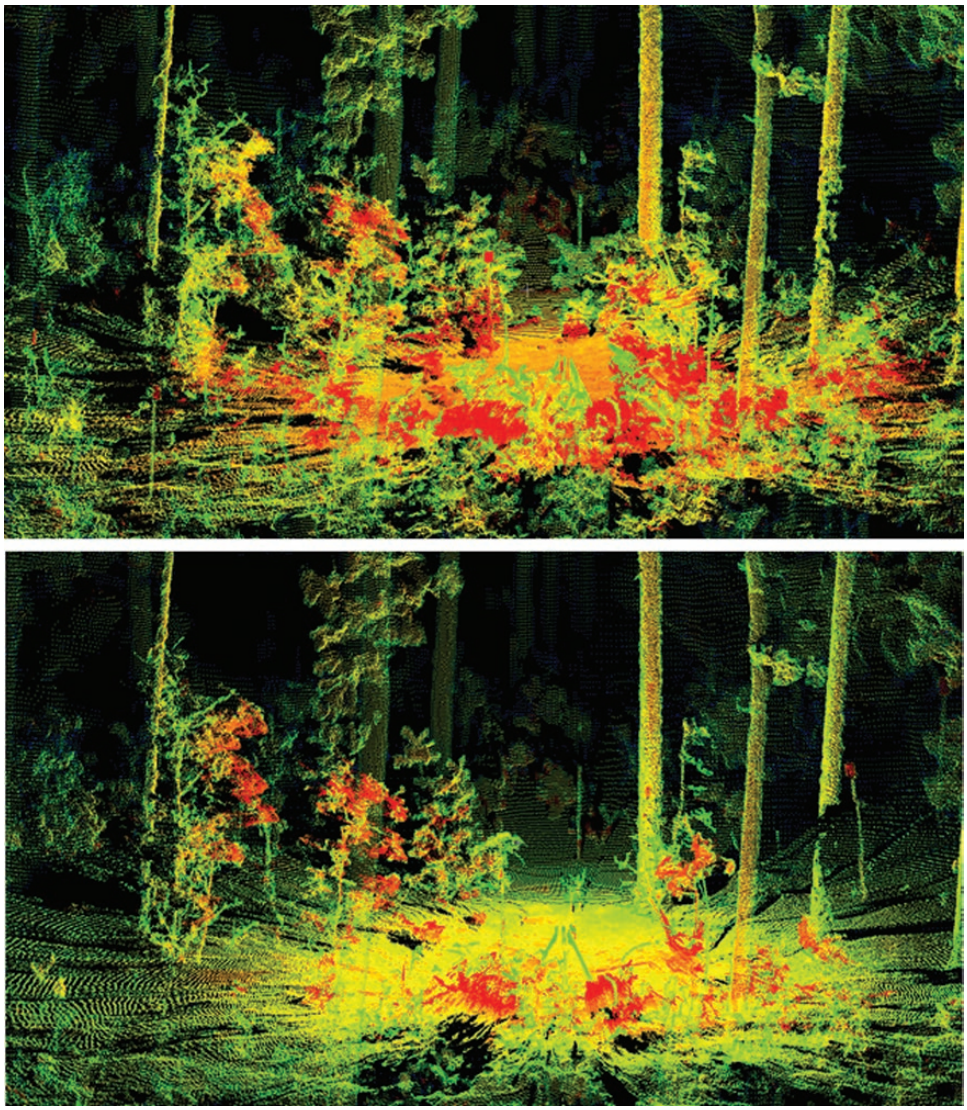

Figure 7. (A) Prefire and (B) postfire terrestrial laser scanning of the predominantly sparkleberry shrub understory vegetation in burn unit 16D1-18. Warmer colors represent higher laser intensity. The tripod on which the terrestrial laser scanner sits is visible at the center of each scene.

Table 2. RMSE in 2D (*x, y*) and 3D (*x, y, z*) for coregistration of treetops in the canopy height model derived from the merged terrestrial laser scanning data collected in 2017–18 to the canopy height model derived from the airborne laser scanning data collected in 2015.

Burn unit	*x, y* RMSE	*x, y, z* RMSE
16D1-17 prefire	0.50	0.98
16D1-17 postfire	0.53	0.81
16D2-17 prefire	0.64	1.15
16D2-17 postfire	0.48	0.74
16D1-18 prefire	0.27	0.90
16D1-18 postfire	0.38	1.07
16D5-18 prefire	0.39	0.71
16D5-18 postfire	0.41	0.67
24A7-18 prefire	0.65	0.80
24A7-18 postfire	0.64	0.86
24B8-18 prefire	0.25	1.06
24B8-18 postfire	0.33	1.13
Mean	0.45	0.91
Standard deviation	0.14	0.17

Note: RMSE, root mean squared error.

Although not included in this study, unmanned aerial vehicle (UAV)-based lidar collections are appealing for "bridging the scale gap" between ALS and TLS data, such as to extract individual tree and crown attributes at the extent of forest stands (Wallace et al. 2014, Mohan et al. 2017). Structure-from-motion (SfM) techniques can be applied to generate photogrammetric point clouds from side-by-side digital aerial photos with high overlap and collected from different view angles (Westoby et al. 2012, Kattenborn et al. 2014, Zarco-Tejada et al. 2014). Photogrammetric points derived using UAV-SfM methods are less accurate and provide less information on understory and surface vegetation/fuel structure relative to the superior canopy penetrability of active lidar sensors with superior penetrability of the overstory canopy (Hodgson and Bresnahan 2004). However, photogrammetric point clouds derived from UAV-SfM and other multi- (or hyper-) spectral images do have the added capacity of three to five (or many) channels and additional information by which fuel (or vegetation) type may be classified (Bright et al. 2016). Because only a small drone and camera are needed to

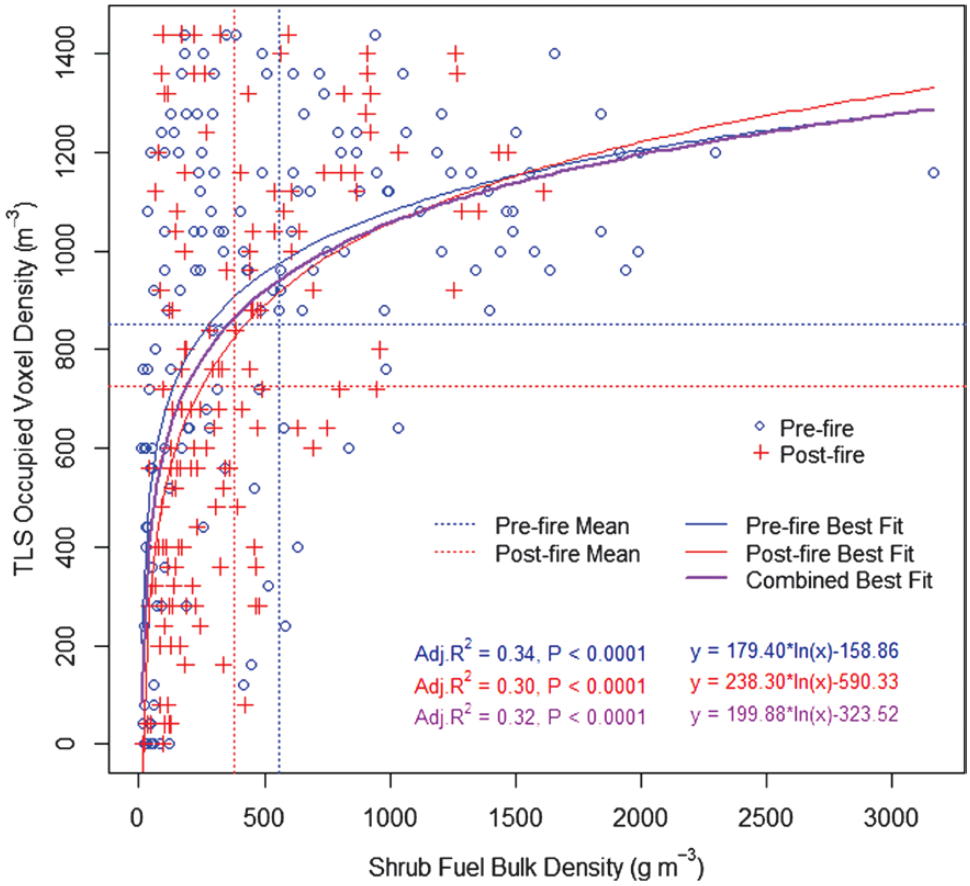

Figure 8. Natural logarithm relations between shrub fuel bulk density measured in 3D shrub sample plots and the density of voxels occupied by terrestrial laser scanning (TLS) points extracted from the point cloud within corresponding virtual *x*, *y*, *z* frames (0.5-m × 0.5-m × 0.1-m intervals). Because the pre- versus postfire functions differed so little, all data were pooled into a single combined equation.

Table 3. Summary statistics of prefire and postfire shrub fuel loads and consumption for the six replicate burn units measured using 2D destructive harvest (traditional) versus 3D non-destructive (point cloud) methods.

Burn unit	2D destructive harvest (traditional)			3D nondestructive terrestrial laser scanning (point cloud)		
	Prefire load (g m^{-2})	Postfire load (g m^{-2})	Consumption (g m^{-2})	Prefire load (g m^{-3})	Postfire load (g m^{-3})	Consumption (g m^{-3})
16D1-17	47.83	162.79	–114.96	106.11	72.44	33.67
16D2-17	2.60	356.30	–353.70	150.85	87.78	63.07
16D1-18	33.63	20.18	13.45	107.62	70.37	37.25
16D5-18	394.54	65.01	329.53	76.55	39.21	37.34
24A7-18	49.32	98.63	–49.32	70.21	47.29	22.92
24B8-18	112.09	91.91	20.18	159.46	127.92	31.54
Mean	106.67	132.47	–25.80	111.80	74.17	37.63
SD	145.48	119.14	221.78	36.93	31.74	13.54
CV	1.36	0.90	–8.59	0.33	0.43	0.36
Min	2.60	20.18	–353.70	70.21	39.21	22.92
Max	394.54	356.30	329.53	159.46	127.92	63.07

Note: CV, coefficient of variation; SD, standard deviation.

create 3D photogrammetric point clouds, UAV-SfM is less costly to acquire than TLS or ALS data. In the future, UAV-mounted lidars could become more available, providing higher point density and added penetrability through the overstory canopy. They could also be more conveniently flown when preferred immediately before or after the fire, whereas contracting an ALS collection is more costly and more logistically difficult to obtain on demand.

Rather than rely on any single sensor, it may be most advantageous to combine datasets, and the information contained therein, from multiple sensors. By merging various point cloud datasets collected at complementary scales and view perspectives (i.e., nadir, oblique, horizontal), the most realistic representations of 3D fuel structure and type may be achieved in the spatial domain. Merging pre- and postfire point clouds may facilitate 3D characterization of the combustible, fine fuel fractions for a more direct estimation of fuel consumption in 3D. Hierarchical, nested sampling provides a tenable framework for upscaling fine-scale (submeter) fuel characterizations at the fine-scale domain of TLS to the tree, stand, and especially landscape domain of fuel- and fire-management decisions (Hudak et al. 2017).

The voxel processing methods used in this study to estimate consumption had two phases. The first phase reduced the point cloud into a 3D array of occupied voxels of 0.001 m^{-3} resolution to map fuels, both pre- and postfire. The second phase tallied the difference in 0.001 m^{-3} occupied voxels between the pre- and postfire 3D fuel maps to map 3D fuel consumption at 1 m^{-3}. This two-phase approach at nested spatial scales is unique to analyze the point cloud, as past TLS or ALS studies to model fuels for surface fires in southern pine forests used the point cloud data directly (e.g., Hudak et al. 2016, Rowell et al. 2016b). We also calculated and tested 3D point density metrics to predict 3D shrub fuel bulk density in this study, but the results were inferior to our model using occupied voxel density as a predictor, because of the problem of duplicated points from merging multiple scans. Thus, the point density was not just a function of the structure of the targeted objects of interest (i.e., shrubs), but confounded by the number of scans, the distance of the TLS from the shrubs, and the presence of occluding objects in between. Removing duplicated points by generating a 3D occupied voxel array dramatically reduced the data volume while also helping to normalize the distribution of point counts reflecting from object surfaces indicative of fuel elements.

This study revealed some important considerations for 3D fuel sampling using a voxel-based approach. Shrub fuels (or other types) are not uniformly distributed within the voxel, so voxels provided only a crude approximation of the 3D fuel elements, which becomes worse as the voxel resolution coarsens. The number of voxels destructively sampled per shrub could be increased, but this would be highly labor-intensive. However, there are analysis tools available to extract object shapes from the point cloud, such as the rLiDAR package (Silva et al. 2015) written in R to extract individual coniferous tree crowns from ALS data (Silva et al. 2016), or potentially scaled down to TLS data of individual shrubs as in this study. Shrubs and deciduous trees often have irregular shapes that exacerbate the problem. Paynter et al. (2016) provided a conceptual framework for reconstructing complex object shapes from TLS data, e.g., using the TreeQSM package (Raumonen 2017). Normalized counts of voxels occupied by TLS (or other point cloud) data within accurately geolocated and delineated 3D object shapes may provide superior training data for predictive fuel models, which could be subsequently applied to voxels for mapping. The 2D analogy already used operationally in lidar-based forestry applications is to bin the ALS point cloud data within typically round forest inventory plots to train predictive models of forest attributes, which are subsequently applied to raster grid cells for mapping. In summary, it would be more efficient to clip and weigh an entire shrub for its biomass after first scanning it to quantify its volume.

Conclusion

Our results reinforce several ideas that motivated this study. First, natural fuelbeds in virtually all fire-prone wildland ecosystems are more complex than what can be realistically characterized using solely traditional 1D (transect) or 2D (plot) methods alone. Spatially explicit measurements are necessary to characterize fuels in 3D for use in physics-based models of fire behavior and, when conducted in pre- and postburn assessments, can be used to map how spatial variability in fuels influences fire behavior, consumption, and postfire vegetation effects. However, complementary destructive sampling is still needed to predict the mass of fuel loads or consumption from metrics derived from the various point cloud datasets. Destructive sampling is also needed to estimate those fuel components (e.g., litter, duff, and fine woody debris fractions) that are not amenable to point cloud characterization because of limited visibility, but that contribute substantially to consumption, energy flux, and emissions.

This study produced two novel findings with regard to estimating shrub fuel consumption. First, the voxel normalization process employed was instrumental to make the TLS point cloud data comparable between scans, including between pre- and postfire scans. Second, it may not be necessary to collect both pre- and postfire destructive samples for model training, since we found only a negligible difference between pre- and postfire predictive fuel models. The significant relations were noisy, however, which in this study may have been only partially remedied by manually adjusting the locations of the 3D shrub plots used for model training. This strongly suggests that survey-grade GNSS accuracy is needed to geolocate small destructive sample plots for model training instead of the resource-grade GNSS used in this study. Further replication and research are needed to test and refine these findings. In particular, testing 3D field sampling of biomass at different scales would prove useful to refine bulk density estimations of other fuel components coupled with 3D point cloud derived volume estimations.

Endnote

1. The use of trade or firm names in this publication is for reader information and does not imply endorsement by the USDA of any product or service.

Literature Cited

Albini, F.A., J.K. Brown, E.D. Reinhard, and R.D. Ottmar. 1995. Calibration of a large fuel burnout model. *Int. J. Wildland Fire* 5(3):173–192.

Andersen, H.-E., T. Clarkin, K. Winterberger, and J. Strunk. 2009. An accuracy assessment of positions obtained using survey-grade global positioning system receivers across a range of forest conditions within the Tanana Valley of Interior Alaska. *West. J Appl. For.* 24:128–133.

Andrews, P.L., C.D. Bevins, and R.C. Seli. 2005. *BehavePlus fire modeling system, version 3.0: User's guide.* USDA Forest Service Gen. Tech. Rep. RMRS-GTR-106WWW, Rocky Mountain Research Station, Ogden, UT. 142 p.

Beaufait, W.R., C.E. Hardy, and W.C. Fischer. 1975. *Broadcast burning in larch–fir clearcuts: The Miller Creek–Newman Ridge Study.* USDA Forest Service, Intermountain Forest and Range Experiment Station, Research Paper INT-175, Ogden, UT.

Blackmarr, W.H., and W.B. Flanner. 1968. *Seasonal and diurnal variation in moisture content of six species of pocosin shrubs.* USDA Forest Service Research Paper SE-33, Southeastern Forest Experiment Station, Asheville, NC.

Bright, B.C., E.L. Loudermilk, S.M. Pokswinski, A.T. Hudak, and J.J. O'Brien. 2016. Introducing close-range photogrammetry for characterizing forest understory plant diversity and surface fuel structure at fine scales. *Can. J. Remote Sens.* 42(5):460–472.

Brown, J.K., E.D. Reinhardt, and W.C. Fischer. 1991. Predicting duff and wood fuel consumption in northern Idaho prescribed fires. *For. Sci.* 37(6):1550–1566.

Byram, G.M. 1959. Combustion of forest fuels. P. 61–89 in *Forest fire: Control and use*, Davis, K.P. (ed.). McGraw-Hill, New York.

Cabo, C., C. Ordoñez, S. García-Cortés, and J. Martínez. 2014. An algorithm for automatic detection of pole-like street furniture objects

from Mobile Laser Scanner point clouds. *ISPRS J. Photogram. Remote Sens.* 87:47–56.

Cabo, C., C. Ordóñez, C.A. López-Sánchez, and J. Armesto. 2018. Automatic dendrometry: Tree detection, tree height and diameter estimation using terrestrial laser scanning. *Int. J. Appl. Earth Observ. Geoinform.* 69:164–174.

Campbell, R.S. 1959. The importance of understory measurement in forest and range research. P. 2–3 in *Techniques and methods of measuring understory vegetation: Proceedings of a Symposium at Tifton, Georgia, October 1958*. USDA Forest Service, Southern Forest Experiment Station and Southeastern Forest Experiment Station, New Orleans, LA.

Davis, K.P. 1959. *Forest fire: Control and use.* 1st ed. McGraw-Hill, New York. 584 p.

Haase, S.M., and S.S. Sackett. 1998. Effects of prescribed fire in giant sequoia–mixed conifer stands in Sequoia and Kings Canyon National Parks. P. 236–243 in *Tall Timbers Fire Ecology Conference Proceedings*, Pruden, T.L., and L.A. Brennan (eds.). Tall Timbers Research Station, Tallahassee, FL. Available online at https://www.fs.usda.gov/treesearch/pubs/43412.

Hawley, C.M., E.L. Loudermilk, E.M. Rowell, and S. Pokswinski. 2018. A novel approach to fuel biomass sampling for 3D fuel characterization. *MethodsX* 5:1597–1604.

Heady, H.F. 1949. Methods of determining utilization of range forage. *J. Range Manag.* 2(2):53–63.

Hedin, A., and T. Turner. 1977. *What is burned in prescribed fire?* Washington Department of Natural Resources Note 16.

Hiers, J.K., J.J. O'Brien, R.J. Mitchell, J.M. Grego, and E.L. Loudermilk. 2009. The wildland fuel cell concept: An approach to characterize fine-scale variation in fuels and fire in frequently burned longleaf pine forests. *Int. J. Wildland Fire* 18:315–325.

Hodgson, M.E., and P. Bresnahan. 2004. Accuracy of airborne lidar-derived elevation: Empirical assessment and error budget. *Photogram. Engineer. Remote Sens.* 70(3):331–339.

Hollis, J.J., S. Matthews, R.D. Ottmar, S.J. Prichard, A. Slijepcevic, N.D. Burrows, B. Ward, K.G. Tolhurst, W.R. Anderson, and J.S. Gould. 2010. Testing woody fuel consumption models for application in Australian southern eucalypt forest fires. *For. Ecol. Manag.* 260:948–964.

Hough, W.A. 1968. *Fuel consumption and fire behavior of hazard reduction burns.* USDA Forest Service Research Paper SE-36, Southeastern Forest Experiment Station, Asheville, NC.

Hough, W.A. 1978. *Estimating available fuel weight consumed by prescribed fires in the South.* Research Paper, USDA Forest Service, Southeastern Forest Experiment Station, Asheville, NC. Available online at https://www.srs.fs.usda.gov/pubs/ja/1978/ja_1978_hough_001.pdf.

Hudak, A.T., M.B. Dickinson, B.C. Bright, R.L. Kremens, E.L. Loudermilk, J.J. O'Brien, B.S. Hornsby, and R.D. Ottmar. 2016. Measurements relating fire radiative energy density and surface fuel consumption—RxCADRE 2011 and 2012. *Int. J. Wildland Fire* 25:25–37.

Hudak, A.T., J.S. Evans, and A.M.S. Smith. 2009. Review: LiDAR utility for natural resource managers. *Remote Sensing* 1:934–951.

Hudak, A.T., R. Ottmar, B. Vihnanek, N. Brewer, A.M.S. Smith, and P. Morgan. 2013. The relationship of post-fire white ash cover to surface fuel consumption. *Int. J. Wildland Fire* 22(6):580–585.

Hudak, A., S. Prichard, R. Keane, L. Loudermilk, R. Parsons, C. Seielstad, E. Rowell, and N. Skowronski. 2017. *Hierarchical 3D fuel and consumption maps to support physics-based fire modeling.* Joint Fire Science Program Project 16-4-01-15 Final Report. 38 p.

Isenburg, M. 2018. *LAStools—efficient tools for LiDAR processing (version 180314, academic).* Available online at http://rapidlasso.com.

Jose, S., E.J. Jokela, and D.L. Miller. 2006. *The longleaf pine ecosystem.* Springer, New York.

Kattenborn, T., M. Sperlich, K. Bataua, and B. Koch. 2014. Automatic single tree detection in plantations using UAV-based photogrammetric point clouds. *Int. Arch. Photogramm. Remote Sens. Spat. Inf. Sci.* 40:139.

Keane, R.E., and K. Gray. 2013. Comparing three sampling techniques for estimating fine woody down dead biomass. *Int. J. Wildland Fire* 22(8):1093–1107.

Keane, R.E., K. Gray, V. Bacciu, and S. Leirfallom. 2012. Spatial scaling of wildland fuels for six forest and rangeland ecosystems of the northern Rocky Mountains, USA. *Landscape Ecol.* 27:1213–1234.

Keeley, J.E. 2009. Fire intensity, fire severity and burn severity: A brief review and suggested usage. *Int. J. Wildland Fire* 18:116–126.

Kreye, J.K., J.M. Varner, and C.J. Dugaw. 2014. Spatial and temporal variability of forest floor duff characteristics in long-unburned Pinus palustris forests. *Can. J. For. Res.* 44:1477–1486.

Lentile, L.B., P. Morgan, A.T. Hudak, M.J. Bobbitt, S.A. Lewis, A.M.S. Smith, and P.R. Robichaud. 2007. Post-fire burn severity and vegetation response following eight large wildfires across the western United States. *Fire Ecol.* 3(1):91–108.

Lewis, S.A., A.T. Hudak, L.B. Lentile, R.D. Ottmar, J.B. Cronan, S.M. Hood, P.R. Robichaud, and P. Morgan. 2011. Using hyperspectral imagery to estimate forest floor consumption from wildfire in boreal forests of Alaska, USA. *Int. J. Wildland Fire* 20:255–271.

Linn, R.R., J. Winterkamp, J.J. Colman, C. Edminster, and J.D. Bailey. 2005. Modeling interactions between fire and atmosphere in discrete element fuelbeds. *Int. J. Wildland Fire* 14:37–48.

Linn, R.R., J. Reisner, J.J. Colmann, and J. Winterkamp. 2002. Studying wildfire behavior using FIRETEC. *Int. J. Wildland Fire* 11:233–246.

Loudermilk, E.L., J.K. Hiers, J.J. O'Brien, R.J. Mitchell, A. Singhania, J.C. Fernandez, W.P. Cropper, and K.C. Slatton. 2009. Ground-based LIDAR: A novel approach to quantify fine-scale fuelbed characteristics. *Int. J. Wildland Fire* 18(6):676–685.

Loudermilk, E.L., J.J. O'Brien, R.J. Mitchell, J.K. Hiers, W.P. Cropper Jr, S. Grunwald, J. Grego, and J. Fernandez. 2012. Linking complex forest fuel structure and fire behavior at fine scales. *Int. J. Wildland Fire* 21:882–893.

Lutes, D.C. 2012. *First order fire effects model mapping tool: FOFEM version 6.0 user's guide.* USDA Forest Service, Rocky Mountain Research Station, Fort Collins, CO.

Mandel, J., S. Amram, J.D. Beezley, G. Kelman, A.K. Kochanski, V.Y. Kondratenko, B.H. Lynn, B. Regev, and M. Vejmelka. 2014. Recent advances and applications of WRF-SFIRE. *Nat. Hazards Earth System Sci.* 14:2829–2845.

Mandel, J., J.D. Beezley, and A.K. Kochanski. 2011. Coupled atmosphere–wildland fire modeling with WRF 3.3 and SFIRE 2011. *Geosci. Model Develop.* 4:591–610.

McCarley, T.R., C.A. Kolden, N.M. Vaillant, A.T. Hudak, A.M.S. Smith, and J. Kreitler. 2017a. Landscape-scale quantification of fire-induced change in canopy cover following mountain pine beetle outbreak and timber harvest. *For. Ecol. Manag.* 391:164–175.

McCarley, T.R., C.A. Kolden, N.M. Vaillant, A.T. Hudak, A.M.S. Smith, B.M. Wing, B.S. Kellogg, and J. Kreitler. 2017b. Multi-temporal LiDAR and Landsat quantification of fire-induced changes to forest structure. *Rem. Sens. Environ.* 191:419–432.

Mell, W., M.A. Jenkins, J. Gould, and P. Cheney. 2007. A physics-based approach to modeling grassland fires. *Int. J. Wildland Fire* 16:1–22.

Mell, W., A. Maranghides, R. McDermott, and S.L. Manzello. 2009. Numerical simulation and experiments of burning Douglas-fir trees. *Combust Flame* 156:2023–2041.

Mitchell, R.J., J.K. Hiers, J.J. O'Brien, S.B. Jack, and R.T. Engstrom. 2006. Silviculture that sustains: The nexus between silviculture, frequent prescribed fire, and conservation of biodiversity in longleaf pine forests of the southeastern United States. *Can. J. For. Res.* 36:2724–2736.

Mohan, M., C.A. Silva, C. Klauberg, P. Jat, G. Catts, A. Cardil, A.T. Hudak, and M. Dia. 2017. Individual tree detection from unmanned aerial vehicle (UAV) derived canopy height model in an open canopy mixed conifer forest. *Forests* 8(9):340.

Mueller, E., N. Skowronski, K. Clark, M. Gallagher, R. Kremens, J. Thomas, M. El Houssami, et al. 2017. Utilization of remote sensing techniques for the quantification of fire behavior in two pine stands. *Fire Safety J.* 91:845–854.

Mutlu, M., S.C. Popescu, C. Stipling, and T. Spencer. 2008. Mapping surface fuel models using lidar and multispectral data fusion for fire behavior. *Rem. Sens. Environ.* 112:274–285.

O'Brien, J.J., E.L. Loudermilk, J.K. Hiers, S. Pokswinski, B. Hornsby, A.T. Hudak, D. Strother, E. Rowell, and B.C. Bright. 2016. Canopy derived fuels drive patterns of in-fire energy release and understory plant mortality in a longleaf pine (*Pinus palustris*) sandhill in Northwest Florida, USA. *Can. J. Remote Sens.* 42(5):489–500.

Olsoy, P., N. Glenn, P. Clark, and D. Derryberry. 2014. Aboveground total and green biomass of dryland shrub derived from terrestrial laser scanning. *ISPRS J. Photogram. Remote Sens.* 88:166–173.

Ottmar, R.D. 2014. Wildland fire emissions, carbon, and climate: Modeling fuel consumption. *For. Ecol. Manag.* 317:41–50.

Ottmar, R.D., T.J. Brown, N.H.F. French, and N.K. Larkin. 2017. *Fire and smoke model evaluation experiment (FASMEE) study plan.* Joint Fire Sciences Program Project 15-S-01-01. 148 p.

Ottmar, R.D., A.T. Hudak, S.J. Prichard, C.S. Wright, J. Restaino, M.C. Kennedy, and R.E. Vihnanek. 2016. Pre- and post-fire surface fuel and cover measurements collected in the southeastern United States for model evaluation and development—RxCADRE 2008, 2011, and 2012. *Int. J. Wildland Fire* 25:10–24.

Ottmar, R.D., R.E. Vihnanek, and J.W. Mathey. 2003. *Stereo photo series for quantifying natural fuels. Volume VIa: Sand hill, sand pine scrub, and hardwoods with white pine types in the Southeast United States with supplemental sites for volume VI.* PMS 838. National Wildfire Coordinating Group, National Interagency Fire Center, Boise, ID. 78 p.

Parsons, R., W.M. Jolly, C. Hoffman, and R. Ottmar. 2016. The role of fuels in extreme fire behavior. Ch. 4. P. 55–82 in *Synthesis of knowledge of extreme fire behavior: Vol. 2 for fire behavior specialists, researchers, and meteorologists.* USDA Forest Service Gen. Tech. Rep. PNW-GTR-891, Pacific Northwest Research Station, Portland, OR. 258 p.

Parsons, R.A., W.E. Mell, and P. McCauley. 2011. Linking 3D spatial models of fuels and fire: Effects of spatial heterogeneity on fire behavior. *Ecol. Model.* 222:679–691.

Parsons, R., L. Wells, F. Pimont, W.M. Jolly, G. Cohn, R. Linn, W. Mell, and C. Hoffman. 2017. Linking FVS to 3D fire models: Introduction to STANDFIRE, a platform for stand scale fuel treatment analysis. In *Proceedings of Forest Vegetation Simulator eConference 2017*. Gen. Tech. Rep, Fort Collins, CO.

Paynter, I., E. Saenz, D. Genest, F. Peri, A. Erb, Z. Li, K. Wiggin, et al. 2016. Observing ecosystems with lightweight, rapid-scanning terrestrial lidar scanners. *Remote Sens. Ecol. Cons.* 19:174–189.

Potter, B.E. 2012. Atmospheric interactions with wildland fire behaviour—I. Basic surface interactions, vertical profiles and synoptic structures. *Int. J. Wildland Fire* 21:779–801.

Prichard, S.J., E. Karau, R.D. Ottmar, C. Wright, J. Cronan, and R. Keane. 2014. A comparison of the Consume and FOFEM fuel consumption models using field data collected in the southeastern United States. *Can. J. For. Res.* 44:784–795.

Prichard, S.J., M.C. Kennedy, C.S. Wright, J.B. Cronan, and R.D. Ottmar. 2017. Predicting forest floor and woody fuel consumption from prescribed burns in southern and western pine ecosystems of the United States. *For. Ecol. Manag.*. 405:328–338.

Prichard, S.J., N.K. Larkin, R.D. Ottmar, N.H.F. French, K. Baker, T. Brown, C. Clements, et al. 2019. The fire and smoke model evaluation experiment—a plan for integrated, large fire–atmosphere field campaigns. *Atmosphere* 10:66.

Prichard, S.J., R.D. Ottmar, and G.K. Anderson. 2007. *CONSUME user's guide and scientific documentation.* Available online at http://www.fs.fed.us/pnw/fera/research/smoke/ consume/consume30_users_guide.pdf [Verified March 7, 2017].

Raumonen, P. 2017. *TreeQSM: Quantitative structure models of single trees from laser scanner data. MATLAB-software TreeQSM User Guide v. 2.30.* 27 p.

R Core Team. 2015. *R: A language and environment for statistical computing.* R Foundation for Statistical Computing, Vienna.

Regional Working Group for America's Longleaf. 2009. Range-wide conservation plan for longleaf pine. Available online at http://americaslongleaf.org/media/86/conservation_plan.pdf.

Reinhardt, E.D., R.E. Keane, and J.K. Brown. 1997. *First order fire effects model: FOFEM 4.0, users guide.* USDA Forest Service Gen. Tech. Rep. INT-GTR-344, Intermountain Research Station, Ogden, UT.

Rowell, E., E.L. Loudermilk, C. Seielstad, and J.J. O'Brien. 2016a. Using simulated 3D surface fuelbeds and terrestrial laser scan data to develop inputs to fire behavior models. *Can. J. Remote Sens.* 42:443–459.

Rowell, E.M., C.A. Seielstad, and R.D. Ottmar. 2016b. Development and validation of fuel height models for terrestrial lidar—RxCADRE 2012. *Int. J. Wildland Fire* 25:38–47.

Sandberg, D.V., and R.D. Ottmar. 1983. Slash burning and fuel consumption in the Douglas-fir subregion. P. 90–93 in *Proceedings, 7th AMS/SAF Conference on Fire and Forest Meteorology.* American Meteorological Society, Boston, MA.

Scholl, E.R., and T.A. Waldrop. 1999. *Photos for estimating fuel loading before and after prescribed burning in the upper coastal plain of the southeast.* USDA Forest Service Gen. Tech. Rep. GTR-SRS-26, Southern Research Station, Asheville, NC.

Seielstad, C.A., and L.P. Queen. 2003. Using airborne laser altimetry to determine fuel models for estimating fire behavior. *J. For.* 101(4):10–15.

Seielstad, C., C. Stonesifer, E. Rowell, and L. Queen. 2011. Deriving fuel mass by size class in Douglas-fir (*Pseudotsuga menziesii*) using terrestrial laser scanning. *Rem. Sens.* 3(12):1691–1709.

Sikkink, P.G., and R.E. Keane. 2012. *Predicting fire severity using surface fuels and moisture.* USDA Forest Service Res. Pap. RMRS-RP-96, Rocky Mountain Research Station, Fort Collins, CO. 37 p.

Silva, C.A., N.L. Crookston, A.T. Hudak, and L.A. Vierling. 2015. *rLiDAR: An R package for reading, processing and visualizing LiDAR (Light Detection and Ranging) data, version 0.1.* Available online at http://cran.rproject.org/web/packages/rLiDAR/index.html; last accessed October 15, 2015.

Silva, C.A., A.T. Hudak, L.A. Vierling, E.L. Loudermilk, J.J. O'Brien, J.K. Hiers, S.B. Jack, et al. 2016. Imputation of individual longleaf pine (*Pinus palustris* Mill.) tree attributes from field and LiDAR data. *Can. J. Remote Sens.* 42(5):554–573.

Smith, A.M.S., and A.T. Hudak. 2005. Estimating combustion of large downed woody debris from residual white ash. *Int. J. Wildland Fire* 14:1–4.

Smith, A.M.S., W.T. Tinkham, D.P. Roy, L. Boschetti, R.L. Kremens, S.S. Kumar, A.M. Sparks, and M.J. Falkowski. 2013. Quantification of fuel moisture effects on biomass consumed derived from fire radiative energy retrievals. *Geophys. Res. Let.* 40:6298–6302.

Southern Forest Experiment Station and Southeastern Forest Experiment Station. 1959. *Techniques and methods of measuring understory vegetation.* USDA Forest Service, New Orleans, LA. 174 p.

Stovall, A.E.L., and H.H. Shugart. 2018. Improved biomass calibration and validation with terrestrial LiDAR: Implications for future LiDAR and SAR missions. *IEEE Trans. Geosci. Remote Sens.* 11:3527–3537.

Stratton, R.D. 2006. *Guidance on spatial wildland fire analysis: Models, tools, and techniques.* USDA Forest Service RMRS-GTR-183, Rocky Mountain Research Station, Fort Collins, CO.

Sullivan, A.L., P.F. Ellis, and I.K. Knight. 2003. A review of radiant heat flux models used in bushfire applications. *Int. J. Wildl. Fire* 12:101–110.

Turner, M.G., W.H. Romme, R.H. Gardner, and W.W. Hargrove. 1997. Effects of fire size and pattern on early succession in Yellowstone National Park. *Ecol. Monog.* 67:411–433.

Urbanski, S. 2014. Wildland fire emissions, carbon, and climate: Emission factors. *For. Ecol. Manag.* 317:51–60.

Valbuena, R., F. Mauro, R. Rodriguez-Solano, and J.A. Manzanera. 2010. Accuracy and precision of GPS receivers under forest canopies in a mountainous environment. *Span. J. Agr. Res.* 8(4):1047–1057.

Van Wagner, C.E. 1972. Duff consumption by fire in eastern pine stands. *Can. J. For. Res.* 2(1):34–39.

Westoby, M.J., J. Brasington, N.F. Glasser, M.J. Hambrey, and J.M. Reynolds. 2012. "Structure-from-Motion" photogrammetry: A low-cost, effective tool for geoscience applications. *Geomorphology* 179:300–314.

Wiggers, M.S., L.K. Kirkman, R.S. Boyd, and J.K. Hiers. 2013. Fine-scale variation in surface fire environment and legume germination in the longleaf pine ecosystem. *For. Ecol. Manag.* 310:54–63.

Wooster, M.J., G. Roberts, G.L.W. Perry, and Y.J. Kaufman. 2005. Retrieval of biomass combustion rates and totals from fire radiative power observations: FRP derivation and calibration relationships between biomass consumption and fire radiative energy release. *J. Geophys. Res. D, Atmos.* 110:D24311.

Wright, C.S. 2013. Fuel consumption models for pine flatwoods fuel types in the southeastern United States. *South. J. Appl. For.* 37(3):148–159.

Zarco-Tejada, P.J., R. Diaz-Varela, V. Angileri, and P. Loudjani. 2014. Tree height quantification using very high resolution imagery acquired from an unmanned aerial vehicle (UAV) and automatic 3D photo-reconstruction methods. *Eur. J. Agron.* 55:89–99.